



# THE FORCED CONVECTION FLOW OF $Ag - Al_2O_3$ HYBRID NANOFUID UNDER THE IMPACT OF EXOTHERMIC REACTION AND THERMAL RADIATION

Ajala A.G<sup>1\*</sup>, Amola B.A.<sup>2</sup>, Asimi Tajudeen<sup>3</sup>, Olaiwola B.O.<sup>4</sup>

<sup>1,2</sup>Department of Mathematics and Statistics, Federal Polytechnic, Ede, Osun State, Nigeria,

<sup>3</sup>Department of Science Laboratory Technology, Federal Polytechnic, Ede, Osun State Nigeria,

<sup>4</sup>Department of Mathematics, Obafemi Awolowo University, Ile Ife, Osun State, Nigeria.

Correspondence email: ajalagbadebo744@gmail.com

**Abstract:** The global hunt for more energy compelled the drive to develop substance with better heat transfer capacity and one major feat in this route is in nano science and technology. Here, the influence of both radiation and activation energy over a moving  $Ag - Al_2O_3$  hybrid nanofluid being considered. The similarity solution to the governing problem was obtained and the numerical solution were obtained using a collocation method following a finite difference approach in MATLAB bvp4c solver. Effects of key parameter on fluid flow, heat and mass transfer rate were presented graphically and discussed.

**Keywords:** Exothermic reaction, hybrid nanofluid, forced convection, radiation.

## 1. Introduction

Fluid stream has different applications in many fields not confined to uses in oil extraction, engine cooling systems, circulation system in the body, drug targeting cleaning of soil from control, water fueled machines, fridges and climate control systems, hydroelectric plants. The mission for headway in each circle of life has required subject matter experts and analysts to foster groundbreaking thoughts and implant these in modern equipment and devices and gadgets utilized in the mechanical, electrical, everyday life and enterprises, for example, climate control systems, fridges, heat exchangers, electronic cooling, vehicle radiators, sun based warm, energy capacity, power through pressure framework and intensity pipes (Gul *et al.*, 2020). Straightforward fluids like water, oil, etc were prior being used for heat conduction and transfer, however it has been understood that this category of fluid have fallen underneath the new world's demand for energy transfer capability.

A huge achievement in energy issue with respect to nano content was kept in 1995 which can be credited to Choi (Choi, 1995). His examination and ensuing deals with what is today known as 'nanofluid' demonstrated that nanofluids relatively shows more warm limit and productivity for heat move rate than straightforward or convectional liquids. Choi and Eastman (1995) thought on improving heat conductivity of fluids with nanoparticles. The likely advantages of nanofluid with copper nanophase materials were talked about and one of such advantages is the drastic decrease in the heat exchanger siphoning power. Thermal vehicle in nanofluids was explored by Eastman *et al.* (2004). Afterward, a survey was made on nanofluid warm conductivity and their heat intensity upgrades by Yu *et al.* (2008). The exergy obliteration of constrained convective nanofluid through a channel with consistent wall temperature was examined by Rezaee and Tayebi (2010). The nuclear power stockpiling execution of Cu/paraffin nanofluids PCMs was mathematically reproduced by Shuying Wu *et al.* (2012). Loganathan *et al.* (2020) thought about the entropy investigation of third - order nanofluid stream on a permeable sheet. Later, the effect of slip on a two - stage stream of Newtonian nanofluid was explored by Ellahi *et al.* (2020).

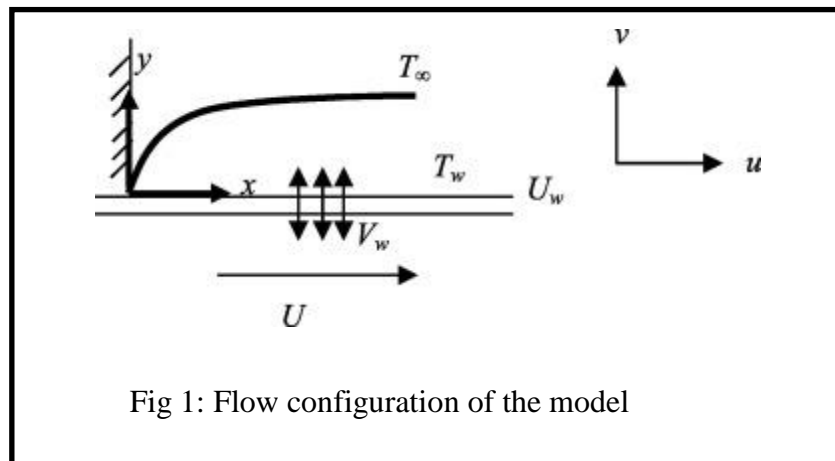
In this era of continuously evolving technology, another adaptation of nanofluid called hybrid nanofluid have recently been developed. Research have shown that the hybrid nanofluid exhibit a higher heat transfer rate and more efficiency than the conventional nanofluids. Unlike the nanofluid, the hybrid nanofluid is

made up of more than one nanoparticle. The properties of hybrid nanofluid and its heat transfer marvel was explored by Suresh *et al.*(2012). Later, Nadeem *et al.* (2018) discussed the importance of hybrid nanofluid over simple nanofluids. The impacts of magnetic dipole on hybrid nanofluid flow was considered by Gul *et al.* (2020). The flow of Cu-Al<sub>2</sub>O<sub>3</sub> hybrid nanofluid fueled by a moving permeable surface was described by Aladdin *et al.*(2020). Rashidi *et al.* (2021) simulated the energy transfer of a hybrid nanosuspension within a heated chamber.

Combustion, heat packs, thermite reactions, manufacturing processes like production of cement, biological processes like respiration, firework and pyrotechnics are few out of numerous important chemical reaction founded processes that involves the release of energy. This kind of chemical reaction which is known as exothermic reaction is characterized by products' energy being lower than the reactants' energy. However, a good understanding of exothermic reaction is essential for maximizing the products of exothermic reactions and based on this, researchers are endeared to investigate this kind of reaction.

A convection flow fueled by exothermic surface reaction was discussed by Chaudhary *et al.*(1995). Monica *et al.* (2017) examined the effects of exothermic reaction in company of heat supply on stagnation point flow of a casson fluid. Koriko *et al.*(2017) investigated exothermic and endothermic reaction for a non-darcian micropolar fluid. The impact of exothermic reaction and viscous dissipation along a curved surface was explored by Ahmad *et al.* (2020). Shehu *et al.*(2022) analysed an exothermic fluid in an heated porous channel. Sharma *et al.*(2022) explored the entropy breeding for an endothermic/exothermic reaction in a mixed convective flow. The magnetic supported exothermic catalytic reaction along a curved surface was analyzed by Muhammad Ashraf *et al.* (2022).

Propelled by every one of the above works, here we have endeavored a numerical examination because of an exothermic reaction and radiation on the constrained convection flow of an hybrid nanofluid with temperature subordinate fluid properties. Utilizing standard similarity variables, the overseeing conditions are changed into an arrangement of normal differential conditions. These acquired conditions are addressed mathematically utilizing matlab bvp5c. The outcomes acquired are introduced in tables and charts and conversations from there on made.



## 2. Mathematical Formulation

Consider a two-dimensional, steady, boundary layer stream of a hybrid nanofluid made up of  $Ag - Al_2O_3$  hybrid nanoparticles with water base fluid past a half infinite plate moving in a uniformly free flow,  $U$  as shown in Fig.1. The system is such that the  $x$ -axis is allied to the plate surface while the

Based on the above assumptions together with ideas from previous works (AbdEl-Gaied and Hamad, 2013; Aladdin *et al.*, 2020, Ahmad *et al.*, 2020), the governing equations for the flow takes the form:

$$\frac{\partial u}{\partial x} + \frac{\partial v}{\partial y} = 0 \tag{1}$$

$$u \frac{\partial u}{\partial x} + v \frac{\partial u}{\partial y} = u_e \frac{du_e}{dx} + \frac{1}{\rho_{hnf}} \frac{\partial}{\partial y} \left( \mu(T) \frac{\partial u}{\partial y} \right) - \frac{\sigma_{hnf} B^2(x)}{\rho_{hnf}} (u - u_e) \quad (2)$$

$$u \frac{\partial T}{\partial x} + v \frac{\partial T}{\partial y} = \frac{1}{(\rho C_p)_{hnf}} \frac{\partial}{\partial y} \left[ k(T) \frac{\partial T}{\partial y} \right] + \beta k_r^2 (T - T_\infty) \left( \frac{T}{T_\infty} \right)^n e^{\left( \frac{-E_a}{k_0 T} \right)} - \frac{1}{(\rho C_p)_{hnf}} \frac{\partial q_r}{\partial y} \quad (3)$$

$$u \frac{\partial C}{\partial x} + v \frac{\partial C}{\partial y} = D_B \frac{\partial^2 C}{\partial y^2} - k_r^2 (C - C_\infty) \left( \frac{T}{T_\infty} \right)^n e^{\left( \frac{-E_a}{k_0 T} \right)} \quad (4)$$

### Subject to the following boundary conditions

$$u = u_w = \delta U_0 x, v = 0, T = T_w, C = C_w, \quad \text{at } y = 0$$

$$u \rightarrow u_e = U_0 x, T \rightarrow T_\infty, C \rightarrow C_\infty, \quad \text{as } y \rightarrow \infty \quad (5)$$

where the component of velocity for  $x$  and  $y$  axes are  $u$  and  $v$  respectively,  $u_e$  denotes the free stream velocity,  $\delta$  is the parameter for plate velocity,  $B$  epitomizes the magnetic parameter,  $\beta$  is the exothermic parameter,  $k$  outlooks the thermal conductivity,  $q_r$  represents the radiative heat flux,  $k_r$  is the chemical reaction rate constant,  $T_\infty$  symbolizes the free stream temperature,  $T_w$  is the wall temperature,  $D_B$  stands for the diffusion coefficient,  $C_\infty$  is the ambient fluid concentration while  $C_w$  is the concentration at the wall and  $\left( \frac{T}{T_\infty} \right)^n e^{\left( \frac{-E_a}{k_0 T} \right)}$  denotes the Arrhenius function. Furthermore, the density of hybrid nanofluid  $\rho_{hnf}$ , viscosity of hybrid nanofluid  $\mu_{hnf}$ , heat capacity of hybrid nanofluid  $(\rho C_p)_{hnf}$ , thermal conductivity of hybrid nanofluid  $K_{hnf}$  are as follow (Hayat and Nadeem 2017, Jawad *et al.*, 2021) and that of relevant nanomaterials are in table 1:

$$\begin{aligned} \rho_{hnf} &= (1 - \omega_2) [(1 - \omega_1) \rho_f + \omega_1 \rho_{s1}] + \omega_2 \rho_{s2}, \quad \mu_{hnf} = \frac{\mu_f}{(1 - \omega_1)^{2.5} (1 - \omega_2)^{2.5}}, \\ (\rho C_p)_{hnf} &= (1 - \omega_2) [(1 - \omega_1) (\rho C_p)_f + \omega_1 (\rho C_p)_{s1}] + \omega_2 (\rho C_p)_{s2}, \\ \sigma_{hnf} &= \frac{2\sigma_{nf} + \sigma_{s2} - 2\omega_2 (\sigma_{nf} - \sigma_{s2})}{2\sigma_{nf} + \sigma_{s2} + \omega_2 (\sigma_{nf} - \sigma_{s2})} \times \frac{\sigma_{s1} + 2\sigma_f - 2\omega_1 (\sigma_f - \sigma_{s1})}{\sigma_{s1} + 2\sigma_f + \omega_1 (\sigma_f - \sigma_{s1})} \times \sigma_f \\ K_{hnf} &= \frac{k_{s2} + 2k_{nf} - 2\omega_2 (k_{nf} - k_{s2})}{k_{s2} + 2k_{nf} + \omega_2 (k_{nf} - k_{s2})} \times \frac{k_{s1} + 2k_f - 2\omega_1 (k_f - k_{s1})}{k_{s1} + 2k_f + \omega_1 (k_f - k_{s1})} \times k_f, \end{aligned} \quad (6)$$

where  $\rho_{s1}, \omega_1, \sigma_{s1}, (\rho C_p)_{s1}, k_{s1}$  are the thermophysical properties for  $Al_2O_3$  nanoparticle,  $\rho_{s2}, \sigma_{s2}, \omega_2, (\rho C_p)_{s2}, k_{s2}$  are the thermophysical properties for silver nanoparticle,  $\rho_f, \mu_f, \sigma_f, (\rho C_p)_f, k_f$  are the thermophysical properties for the base fluid.

The Roseland approximation for radiation (Zaib *et al.*, 2018) is given as:

$$q_r = - \frac{4\sigma^* \partial T^4}{3k^* \partial y} \quad (7)$$

This is solved using Taylor's series and higher order terms neglecting higher order terms, thus the radiation term in equation (3) gives

**Table 1:** Thermophysical Properties of some nanofluids (Mekheimer *et al.*, 2018; Khan *et al.* 2020)

Material	Density $\rho$ ( $kg/m^3$ )	Specific Heat Capacity $C_p$ ( $J/KgK$ )	Electrical Conductivity $\sigma$ ( $S/m$ )	Thermal Conductivity $K$ ( $W/mk$ )
Water	977	4180	$2.1 \times 10^{-4}$	0.607
Silver ( <i>Ag</i> )	10500	235	18.9	429
Aluminium Oxide ( $Al_2O_3$ )	3690	773	$0.85 \times 10^{-5}$	40

$$\frac{\partial q_r}{\partial y} = \left( -\frac{16\sigma^* T_\infty^3}{3k_1} \frac{\partial^2 T}{\partial y^2} \right) \quad (8)$$

Introducing well established variables [Shehzardet *et al.*, 2015; Mohammed *et al.*,2016; Prasad *et al.* 2010; Animasaun 2015, Ajayi et al, 2017] of the form

$$\theta(\eta) = \frac{T - T_\infty}{T_w - T_\infty}, \quad \phi(\eta) = \frac{C - C_\infty}{C_w - C_\infty}, \psi = \sqrt{\vartheta U_0} x f(\eta), \quad \eta = y \sqrt{\frac{U_0}{\vartheta}}, \quad u = \frac{\partial \psi}{\partial y}, v = \frac{\partial \psi}{\partial x} \quad (9)$$

In addition, the fluid viscosity and thermal conductivity are taken to be linear utility of temperature in the form

$$\mu(T) = \mu^* [1 + b(T_w - T)], k = K [1 + \gamma(T - T_\infty)] \quad (10)$$

Juxtaposing equations (1) – (5) with variables(8) – (10),the continuity equation (1) is automatically satisfied and the other equations reduces to theform:

$$\left[ \frac{(a + (1 - \theta)\xi)}{(1 - \omega_1)^{2.5}(1 - \omega_2)^{2.5} \left\{ (1 - \omega_2) \left[ (1 - \omega_1) + \frac{\omega_1 \rho_{s1}}{\rho_f} \right] + \frac{\omega_2 \rho_{s2}}{\rho_f} \right\}} \right] \frac{d^3 f}{d\eta^3} - \frac{\xi}{(1 - \omega_1)^{2.5}(1 - \omega_2)^{2.5} \left\{ (1 - \omega_2) \left[ (1 - \omega_1) + \frac{\omega_1 \rho_{s1}}{\rho_f} \right] + \frac{\omega_2 \rho_{s2}}{\rho_f} \right\}} \frac{d^2 f}{d\eta^2} \frac{d\theta}{dy} - \frac{df}{d\eta} \frac{df}{d\eta} + f(\eta) \frac{d^2 f}{d\eta^2} + 1 - \frac{Ha}{\left\{ (1 - \omega_2) \left[ (1 - \omega_1) + \frac{\omega_1 \rho_{s1}}{\rho_f} \right] + \frac{\omega_2 \rho_{s2}}{\rho_f} \right\}} \left( \frac{df}{d\eta} - 1 \right) = 0 \quad (11)$$

$$\frac{3R_a(1 + \theta\epsilon) + 4}{3R_a \left[ (1 - \omega_2) \left[ (1 - \omega_1) + \frac{\omega_1(\rho C_p)_{s1}}{(\rho C_p)_f} \right] + \frac{\omega_2(\rho C_p)_{s2}}{(\rho C_p)_f} \right]} \frac{d^2 \theta}{d\eta^2} + Pr f(\eta) \frac{d\theta}{d\eta} + \frac{\epsilon}{\left[ (1 - \omega_2) \left[ (1 - \omega_1) + \frac{\omega_1(\rho C_p)_{s1}}{(\rho C_p)_f} \right] + \frac{\omega_2(\rho C_p)_{s2}}{(\rho C_p)_f} \right]} \frac{d\theta}{d\eta} \frac{d\theta}{d\eta} + Pr \beta C_r \theta (1 + T_d \theta)^n e^{\left( \frac{-E_1}{(1 + T_d \theta)} \right)} = 0 \quad (12)$$

$$\frac{d^2\phi}{d\eta^2} + S_c f(\eta) \frac{d\phi}{d\eta} - S_c C_r \phi (1 + T_d \theta)^n e^{\left(\frac{-E_1}{(1+T_d\theta)}\right)} = 0 \quad (13)$$

**Subject to the boundary conditions**

$$\frac{df(0)}{d\eta} = \delta, \quad f(0) = 0, \quad \theta(0) = 1, \quad \phi(0) = 1,$$

$$\frac{df(\infty)}{d\eta} \rightarrow 1 \quad \theta(\infty) \rightarrow 0, \quad \phi(\infty) \rightarrow 0 \quad (14)$$

Where Chemical reaction parameter  $C_r = \frac{k_r^2}{U_0}$ , activation energy parameter  $E_1 = \frac{E_a}{k_0 T_\infty}$ , Local magnetic parameter  $H_a = \frac{\sigma B^2}{\rho_f U_0}$ , Temperature dependent thermal conductivity parameter  $\epsilon = \gamma(T_w - T_\infty)$ , Temperature dependent viscosity parameter  $\xi = b(T_w - T_\infty)$ , Schmidt number  $S_c = \frac{\vartheta}{D_B}$ , Prandtl number  $P_r = \frac{(\rho c_p)_f \vartheta}{K_f}$ , Radiation parameter  $R_a = \frac{k_f k_1}{4\sigma^* T_\infty^3}$ , temperature difference parameter  $T_d = \frac{(T_w - T_\infty)}{T_\infty}$ . The physical qualities of engineering interest in this study are the skin friction coefficient  $c_f$ , local Nusselt number  $Nu_f$  and Sherwood number  $Sh$  which are defined as

$$C_f = \frac{\tau_w}{\rho_f U^2}, \quad Nu_x = \frac{x q_w}{k_f (T_w - T_\infty)}, \quad Sh = \frac{x J_w}{D(C_w - C_\infty)} \quad (15)$$

$$\text{and } \tau_w = \mu_{hnf} \left(\frac{\partial u}{\partial y}\right)_{y=0}, \quad q_w = -k_{hnf} \left(\frac{\partial T}{\partial y}\right)_{y=0} + (q_r)_{y=0}, \quad J_w = -D_B \left(\frac{\partial C}{\partial y}\right)_{y=0} \quad (16)$$

### 3. Numerical Solution

The coupled ordinary differential equations (11) – (13) and their corresponding boundary conditions (14) are first reduced to a system of first order equations using the method of superimposition (Na, 1979) using the identities:

$$f = f_1, \frac{df}{d\eta} = f_2, \frac{d^2f}{d\eta^2} = f_3, \theta = f_4, \frac{d\theta}{d\eta} = \theta' = f_5, \frac{d^2\theta}{d\eta^2} = f_5', \phi = f_6, \frac{d\phi}{d\eta} = f_6', \frac{d^2\phi}{d\eta^2} = f_7 \quad (17)$$

The obtained system of equations are thereafter solved numerically using a finite difference like collocation code in Matlab `bvp5c` o.d.e. solver.

### 4. Results and Discussion

Numerical computation has been carried out for various values of activation energy parameter ( $E_1$ ), Chemical reaction parameter ( $C_r$ ), Hartmann number ( $H_a$ ), Schmidt number ( $S_c$ ), Prandtl number ( $P_r$ ), Radiation parameter ( $R$ ), temperature difference parameter ( $T_d$ ), thermal conductivity parameter ( $\epsilon$ ), velocity parameter ( $\delta$ ) and volume fraction parameter ( $\omega$ ) using the numerical scheme discussed in the previous section. The numerical values obtained from the result are plotted in Figures 2 – 11 for  $\beta = 0.2$ ,  $P_r = 0.7$ ,  $\delta = 0.4$ ,  $C_r = 1$ ;  $\beta = 0.2$ ,  $\xi = 0.7$ ,  $\epsilon = 0.7$ ,  $Pr = 0.7$ ,  $Ra = 1$ ,  $H_a = 1$ ,  $S_c = 0.22$ ,  $T_d = 0.7$ ,  $E_1 = 1$ ,  $n = 1$  except otherwise stated. Figure 2 illuminates the variation in temperature instigated by a change in thermal conductivity parameter. The figure revealed that temperature increase as thermal conductivity

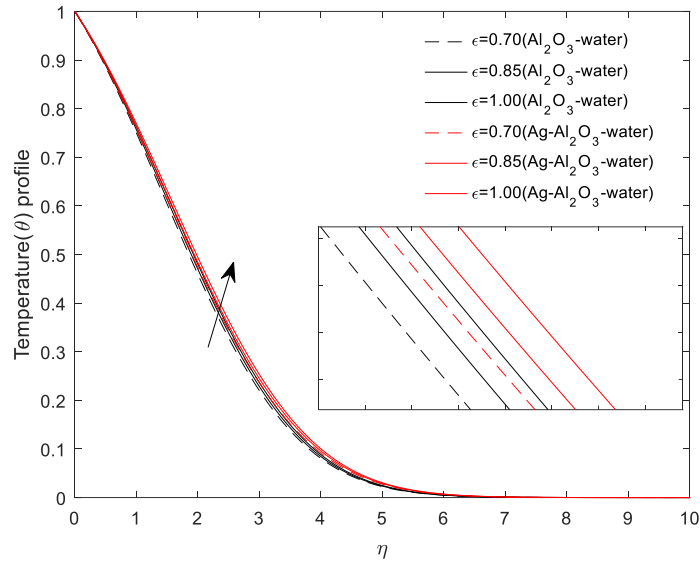


Figure 2: Variation in Thermal conductivity parameter with Temperature

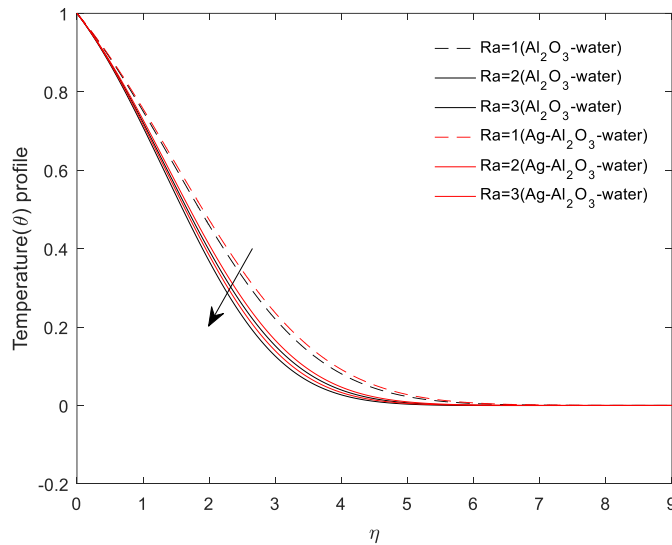


Figure 3: Variation in Radiation parameter with Temperature

parameter increases. This observation is in harmony with Figure 6 reported by Hazarika and Konch Jadav (2014). Figure 3 illustrates the effect of radiation parameter on temperature. The figure demonstrated that radiation causes a drop in temperature. This behavior is in harmony with Figure 7 reported by Abdul Maleque (2013). The effect of Arrhenius parameter ( $E_1$ ) on fluid heat sensation is elucidated in Figure 4. It can be noted that the Arrhenius parameter leads to a decline in temperature.

Figure 5 shows the influence of temperature difference on concentration profile. The figure showed that fluid concentration reduces for increase in temperature difference.

Effect of chemical reaction parameter on temperature is elucidated in Figure 6. The figure demonstrated that chemical reaction spark a rise in fluid temperature. This behavior is in harmony with Figure 21 reported by Animasaun (2015). The impact of chemical reaction parameter on concentration is demonstrated in Figure 7.

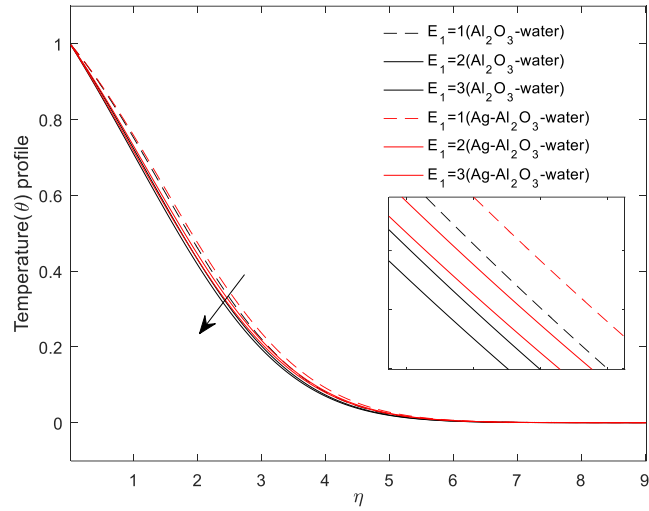


Figure 4: Variation in Arrhenius parameter( $E_1$ ) with Temperature

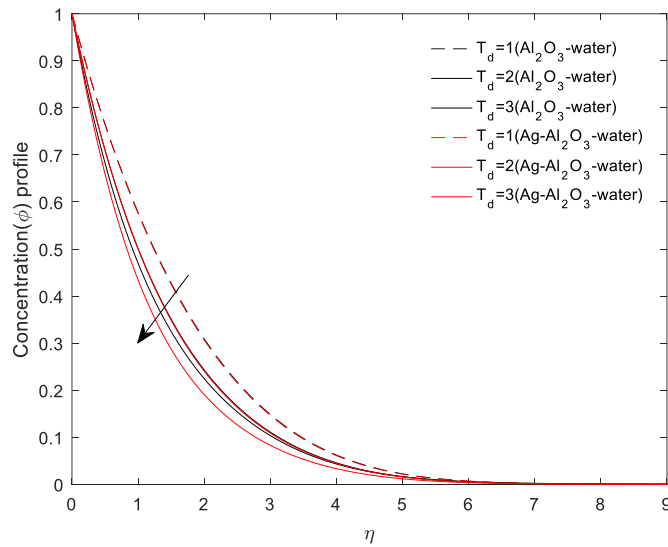


Figure 5: Variation in temperature difference parameter( $T_d$ ) with concentration

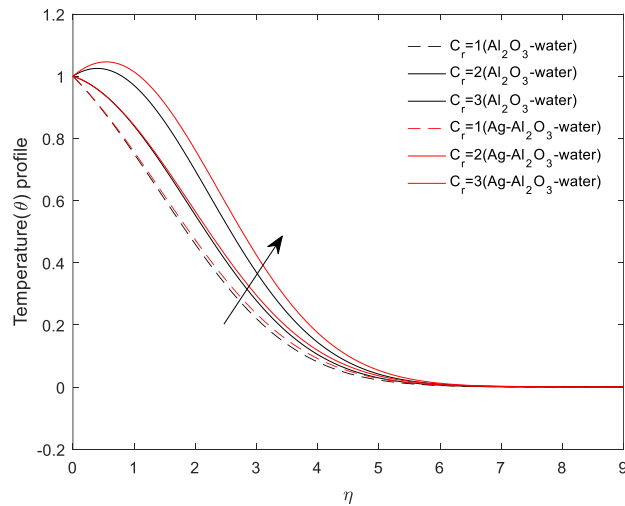


Figure 6: Variation in Chemical Reaction parameter ( $C_r$ ) with Temperature

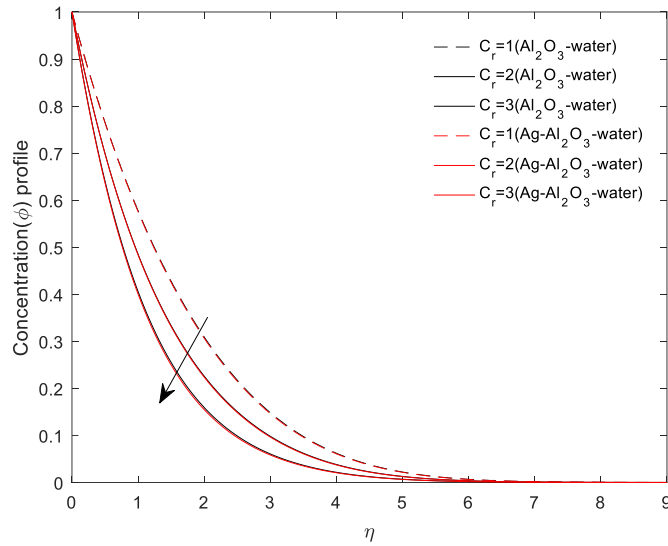


Figure 7: Variation in Chemical Reaction parameter ( $C_r$ ) with Concentration

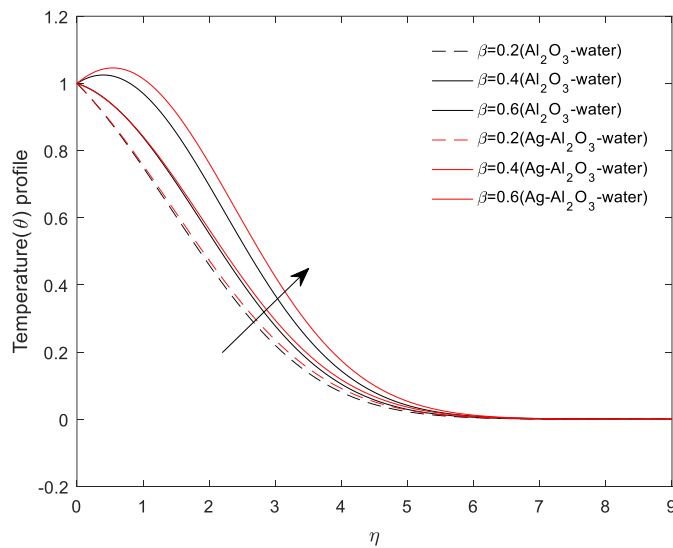


Figure 8: Variation in Exothermic parameter ( $\beta$ ) with Temperature

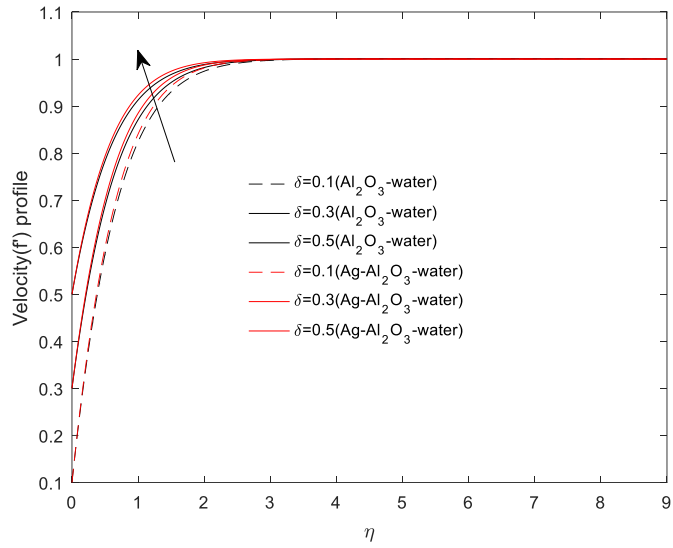


Figure 9: Variation in velocity parameter ( $\delta$ ) with velocity

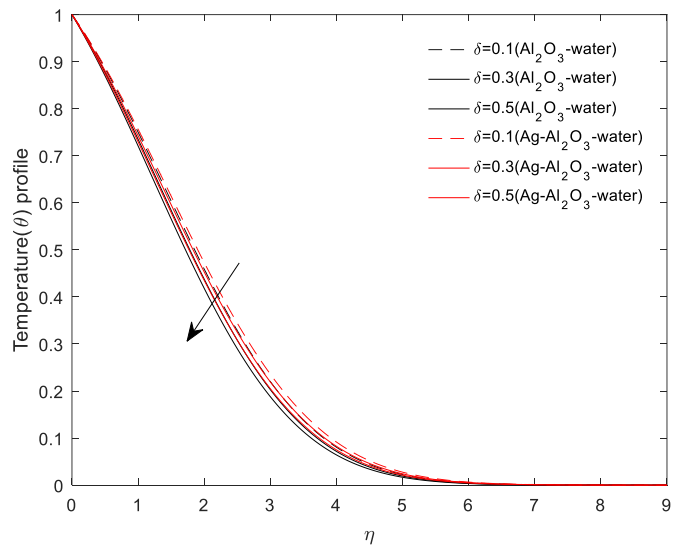


Figure 10: Variation in velocity parameter ( $\delta$ ) with Temperature

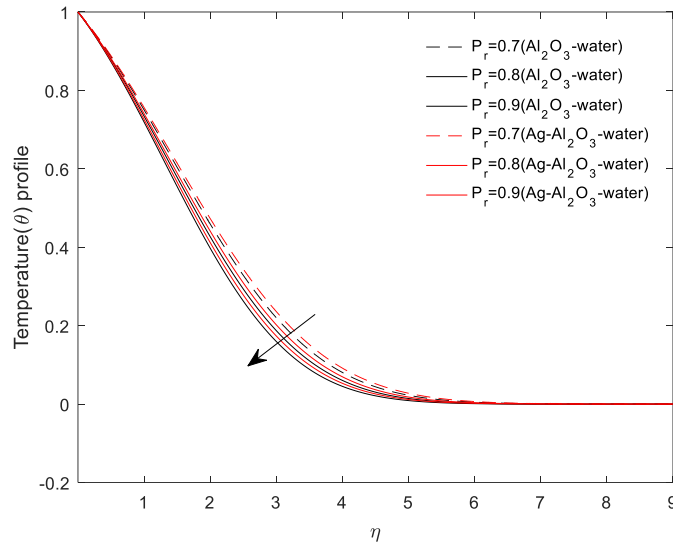


Figure 11: Effect of Prandtl number on Temperature

Concentration profile is a decreasing function of chemical reaction. This is in accord with Figure 20 by Animasaun (2015). The variation in exothermic parameter with temperature is shown in Figure 8. The figure illuminated that temperature increases with exothermic parameter. This behavior is due to the fact that in exothermic reaction heat is released and so by increasing this parameter means more of such reaction which commulates to more heat into the system. Impact of Velocity parameter on velocity profile is shown in figure 9. The figure pictured fluid velocity as an increasing function of velocity parameter. The underlining reason for this behavior is due to the fact that the velocity parameter is a direct function of the plate velocity and as such, increasing this parameter translate to increasing plate velocity which will invariably enhance fluid flow. Figure 10 elucidated the variation of velocity parameter with temperature and the figure revealed that the parameter causes a decline in fluid temperature.

Figure 11 portrayed the impact that Prandtl number parameter have on fluid temperature. The figure displayed that temperature reduces for rising Prandtl number and this is because Prandtl number is inversely proportional to fluid thermal conductivity while thermal conductivity is a direct function of temperature, hence the resulting decrease in temperature. In each of the figures, the influence of selected parameters where comparatively shown for both  $Al_2O_3$  nanofluid and the hybrid version ( $Ag - Al_2O_3$ ). The hybrid version showed better response to variations in parameters in most of these figures.

## 6. Conclusion

The analysis of various parameters for the steady laminar forced convection flow of an incompressible, electrically conducting hybrid nanofluid has been carried out. The following were detected:

- i. Velocity parameter enhances fluid flow but causes a decline in fluid temperature.
- ii. Fluid temperature increases for a rise in any of thermal conductivity, chemical reaction and exothermic constraints while a decline is experienced due to radiation, velocity parameter, Prandtl number and Arrhenius parameter.
- iii. Concentration distribution is a decreasing function of each chemical reaction and temperature difference.
- iv. The hybrid duo of  $Ag - Al_2O_3$  shows better response to variation in parameters than a single nano item.

- v. Thermal conductivity parameter and the Prandtl number cause a rise in the Nusselt number while Prandtl number reduces Sherwood number.

## References

- Ahmad U., Ashraf M., Khan I. and Nisar K.S. (2020). Modelling and Analysis of the Impact of Exothermic Catalytic Chemical Reaction and Viscous Dissipation on Natural Convection Flow Driven along a Curved Surface. *Thermal Science* : Vol. 24, Suppl. 1, pp. S1 – S11.
- Ajayi TM, Omowaye AJ, Animasaun I.L.(2017). Viscous Dissipation Effects on the Motion of Casson Fluid over an Upper Horizontal thermally stratified Melting Surface of a Paraboloid of Revolution: Boundary layer Analysis. *Journal of Applied Mathematics*, Volume 2017, Article ID 1697135.
- Aladdin N.A.L., Bachok N. and Pop I. (2020). Cu-Al<sub>2</sub>O<sub>3</sub>/water hybrid nanofluid flow over a permeable moving surface in presence of hydromagnetic and suction effects, *Alexandria Engineering Journal* 59, 657 – 666.
- Animasaun I.L. (2015). Effects of thermophoresis, variable viscosity and thermal conductivity on free convective heat and mass transfer of non-darcian MHD dissipative Casson fluid flow with n<sup>th</sup> order chemical reaction, *Journal of Mathematical Society* 34(2015):11 – 31.
- Choi S.U.S. (1995). Enhancing thermal conductivity of fluids with nanoparticles, ASME-Publicat Fe, 231: 99 – 106.
- Choi S.U.S. and Eastman J.A. (1995). Enhancing thermal conductivity of fluids with nanoparticles, article, October 1, Illinois, University of North Texas Libraries, UNT Digital Library.
- Eastman, J. A., Phillpot, S. R., Choi, S. U. S. and Keblinski, P. (2004). Thermal Transport in Nanofluids, *Annual Review of Materials Research*, 34(1), 219– 246.
- Ellahi R., Hussain F., Asad Abbas S., Sarafraz M.M., Goodarzi M., Shadloo M.S. (2020). Study of Two-Phase Newtonian Nanofluid Flow Hybrid with Hafnium Particles under the Effects of Slip, *Inventions*. 5(1):6.
- Gul T., Bilal M, Khan A, AedhAlreshidi N., Mukhtar S, Shah Z. and Kumam P. (2020). Magnetic Dipole impact on Hybrid nanofluid Flow over an Extending Surface, *Scientific Reports (Nature Publisher Group)*.
- Hayat T., Nadeem S. (2017). Heat transfer enhancement with Ag–CuO/ water hybrid nanofluid, *Results Phys* 7, 2317–2324.
- Hazarika G.C., Konch Jadav(2014). Effects of Variable Viscosity and Thermal Conductivity on MHD Free Convective Flow along a Vertical Porous Plate with Viscous Dissipation, *International Journal of Mathematics Trends and Technology*, 15 Number 1, ISSN: 2231-5373.
- Jawad M., Saeed A, Tassaddiq A, Khan A., Gul T. Kuman P., Shah Z. (2021). Insight into the dynamics of Second Grade Hybrid Radiative Nanofluid Flow with the Boundary Layer Subject to Lorentz Force, *Scientific Reports*, 11, 4894, Doi.org/10.1038/s41598-021-84144-6.
- Jha, B.K., Samaila, G. (2020). Thermal radiation effect on boundary layer over a flat plate having

- convective surface boundary condition, *SN Appl. Sci.* 2, 381 (2020).
- Khan U, Shafiq A, Zaib A, Sherif El-Sayed M., Beleanu D (2020). MHD radiative Blood Flow embracing Gold Particles iva a Slippery Sheet through an Erratic Heat Sink/Source. *Mathematics*, 8, 1597;
- Loganathan K., Muhiuddin G., Alanazi A.M., Fehaid S. Alshammari, Bader M. Alqurashi and Rajan S. (2020). Entropy Optimization of Third-Grade Nanofluid Slip Flow Embedded in a Porous Sheet With Zero Mass Flux and a Non-Fourier Heat Flux, *Model. Front. Phys.*, 24 November 2020.
- MekheimerKh.S., Hasona W.M., Abo-Elkhair R.E., Zaher A.Z. (2018). Peristaltic Blood Flow with Gold Nanoparticles as a Third Grade Nanofluid in Catheter: Application of Cancer Therapy, *Physics Letters A* 382, 85–93
- Na T.Y., *Computational Methods in Engineering Boundary Value Problems*, New York (1979): Academic Press.
- Nadeem, S., Abbas, N. & Khan, A. U. (2018). Characteristics of three dimensional stagnation point flow of Hybrid nanofluid past a circular cylinder, *Results in physics* 8, 829–835.
- Prasad K.V., Vajravelu K., Datti P.S. (2010). The effects of variable fluid properties on the hydromagnetic flow and heat transfer over a non-linearly stretching sheet. *Int. J. Ther. Sci.*, 49603-10.
- Rashidi, M.M., Sadri, M.; Sheremet, M.A. (2021). Numerical Simulation of Hybrid Nanofluid Mixed Convection in a Lid-Driven Square Cavity with Magnetic Field Using High-Order Compact Scheme, *Nanomaterials*(2021), 11, 2250.
- Rezaee, F.K. and Tayebi A. (2010). Exergy Destruction of Forced Convective (Ethylene glycol+alumina) Nanofluid through a Duct with constant wall Temperature in contrast to (ethylene glycol) fluid. *Journal of Applied Sciences*, 10, 1279 – 1285.
- Shuying Wu, Hua Wang, Song Xiao, Dongsheng Zhu (2012). Simulation on Thermal Energy Stored Behavior of Cu/paraffin nanofluids PCMs. *Procedia Engineering* 31(2012) 240 – 244.
- Suresh, S., Venkataraj, K. P., Selvakumar, P. and Chandrasekar, M.(2012). Effect of Al<sub>2</sub>O<sub>3</sub>-Cu/water hybrid nanofluid in heat transfer. *Experimental Thermal and Fluid Science* 38, 54–60 (2012).
- Yu W., France D.M., Routbort J.L. and Choi S.U. S.(2008). Review and Comparison of Nanofluid Thermal Conductivity and Heat Transfer Enhancements. *Heat Transfer Engineering* Volume 29, 2008 - Issue 5.
- Zaib A., Chamkha A. J., Rashidi M. M., and Bhattacharyya K.(2018). Impact of nanoparticles on flow of a special non-Newtonian third-grade fluid over a porous heated shrinking sheet with nonlinear radiation. *Nonlinear Engineering* 7(2): 103– 111.
- AbdulMaleque Kh. (2013). Effects of Exothermic/Endothermic Chemical Reactions with Arrhenius Activation Energy on MHD Free Convection and Mass Transfer Flow in Presence of Thermal Radiation. *Journal of Thermodynamics* Volume 2013, Article ID 692516.
- Monica M., Sucharitha J. and Kishore Ch.(2017). Effects of Exothermic chemical Reaction with Arrhenius

Activation Energy, non-uniform heat source/sink on MHD Stagnation point Flow of a Casson Fluid over a non-linear Stretching Sheet with variable fluid properties and slip conditions. *Journal of Nigerian Mathematical Society*, 36, 163 – 190.

Shehu M.Z, Abdullahi M., Umar M. (2017). MHD Slip flow of an Exothermic Fluid in a Convectively Heated porous Vertical Channel. *Saudi Journal of Engineering and Technology*. 7(10):542 – 549.

Chaudhary M. A., Linan A. and Merkin J. H. (1995). Free convection boundary layers driven by exothermic surface reactions: critical ambient temperatures *Math. Engng. Ind.*, Vol. 5, No. 2, pp. 129-145.

Koriko O.K., Omowaye A.J, Animasaun I.L.(2017). Boundary layer Analysis of Exothermic and Endothermic kind of Chemical Reaction in the flow of a non-Darcian Unsteady Micropolar Fluid along an infinite Vertical Surface. *International Journal of Engineering Research in Africa*, 8, 90 – 101.

Sharma B.K., Gandhi R, Mishra N. and Al-Med Qasem M.(2022). Entropy generation minimization of higher order endothermic/exothermic chemical reaction with activation energy for MHD mixed convective flow on a stretching surface. *Scientific Reports* 2022, 12, 17688.

Muhammad Ashraf,Uzma Ahmad, Saqib Zia, Rama Suba Gorla, Amnah S. Al-Johani, Ilyas Khan, Mulugeta Andeuaem(2022). Magneto-Exothermic Catalytic Chemical Reaction along a curved surface. *Mathematical Problems in Engineering*, 2022, Article ID 8439659.